

# Oxidative trends of TiO<sub>2</sub>—Hole trapping at anatase and rutile surfaces<sup>†</sup>

Paweł Zawadzki,<sup>\*a§</sup> Anders Bo Laursen,<sup>b</sup> Karsten Wedel Jacobsen,<sup>a</sup> Søren Dahl<sup>b</sup> and Jan Rossmeisl<sup>a</sup>

## Supplemental Material

### Self-trapping energies in surface layers

Strong electron interaction with lattice distortion can lead to electron self-trapping, i.e. formation of a localized bound state. The self-trapping energy is defined as a difference between the energy of the delocalized state at zero distortion (perfect lattice)  $E_D(\mathbf{Q} = \mathbf{0})$  and the energy of the localized (trapped) state at its equilibrium distortion  $E_T(\mathbf{Q} = \mathbf{Q}_T)$ . In surface layers the self-trapping energy depends both on the type of surface termination  $S$  and the exact location of the trapping site  $z$ :

$$\varepsilon_T(S, z) = E_T(\mathbf{Q}_T; S, z) - E_D(\mathbf{Q} = \mathbf{0}; S). \quad (1)$$

In order to position such trapping level in the band gap common reference energy is needed as the energy of the delocalized state can be different for different surface terminations and the bulk band edges are not well defined for a finite thickness surface slab. Using the fact that at large depth below the surface the self-trapping energy must converge to the value in the bulk:

$$\lim_{z \rightarrow \infty} \varepsilon_T(S, z) = \varepsilon_T^B, \quad (2)$$

we find that the electron (hole) self-trapping level relative the conduction (valence) band maximum in the bulk takes the form:

$$\varepsilon_T(S, z) = \varepsilon_T^B + E_T(\mathbf{Q}_T; S, z) - E_T(\mathbf{Q}_T; S, z \rightarrow \infty). \quad (3)$$

In Ref.<sup>1</sup> we calculated  $\varepsilon_T^B$  to be 0.05 eV and 0.2 eV for rutile and anatase, respectively. To calculate  $E_T(\mathbf{Q}_T; S, z \rightarrow \infty)$  we average  $\Delta$ -SCF energy  $E_T(\mathbf{Q}_T; S, z)$  of the four [two in case of anatase (100)] most deeply positioned relative to surface hole states in a unit cell sufficiently large for  $E_T(\mathbf{Q}_T; S, z)$  to show convergence behaviour. Fig. 1 and Fig. 3 show self-trapping energy profiles aligned with the self-trapping energy in the bulk. In Fig. 5 we plot the self-trapping energy profiles for different unit cell sizes.

### Delocalization Error

Calculation of self-trapping energies with semi-local exchange-correlation DFT, such as PBE DFT, is problematic as the method tends to favour energetically delocalized states—the infamous many electron self-interaction<sup>2</sup> or

delocalization error<sup>3</sup>. In Eq. 3 the only term where the energy difference between delocalized and localized state is calculated is the bulk self-trapping energy  $\varepsilon_T^B$ . We assume that the energy differences between localized states are correct and take the value of the bulk hole self-trapping energy corrected for the delocalization error from Ref.<sup>1</sup>. We further note that the relative self-trapping energies for different facades of one phase are independent on the choice of reference energy as it only shifts the self-trapping energies by a constant.

### Modeling self-trapped hole with $\Delta$ -SCF

The linear expansion  $\Delta$ -SCF is an approximate technique to calculate excited state energies that uses<sup>4</sup>

- ground state energy functional,
- approximate excited state density.

The excited state density is constructed by adding or subtracting the density of an orbital  $|\phi\rangle$  expanded in KS states while conserving the total number of electrons:

$$\rho(r) = \sum_n f_{N\pm 1}(\varepsilon_n) |\psi_n(\vec{r})|^2 \mp |\psi(\vec{r})|^2 \quad (4)$$

where  $f$  is Fermi-Dirac distribution and

$$|\psi\rangle = \sum_n \langle \psi_n | \phi \rangle |\psi_n\rangle. \quad (5)$$

The Kohn-Sham equations are then solved till self-consistently is achieved.

The difficult part in application of  $\Delta$ -SCF is choice of the orbital  $|\phi\rangle$  that will lead to excited state density. A physical insight into the nature of the excited state is necessary.

To construct localized hole state in TiO<sub>2</sub> we use the oxygen  $p$ -like orbital<sup>1</sup> perpendicular to the OTi<sub>3</sub> building block of TiO<sub>2</sub>. As discussed in Ref.<sup>1</sup> such choice is consistent with experimental EPR data, electronic structure and symmetry arguments. With electron density constrained by Eq. 4 and Eq. 5 (the expansion is over the states below the Fermi level) we relaxed electronic and atomic structures. Convergence of the energy and the maximum force of 0.05 eV/Å was achieved in most cases. In some, however, the hole is unstable and the above convergence criterion has not been attained therefore there we report local minima. These does not change the overall picture as unstable states do not trap holes.

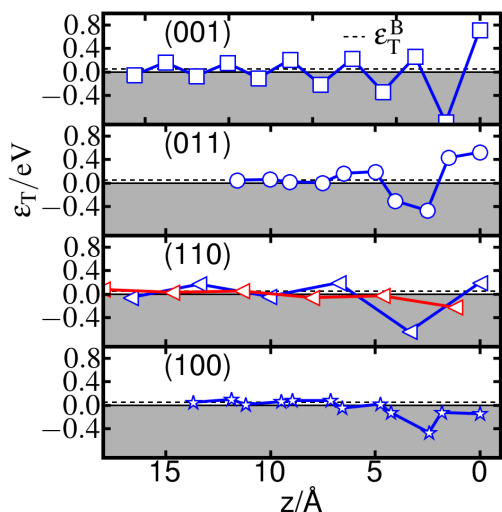


**Fig. 1** Self trapping energies  $\epsilon_T$  with respect to the valence band edge for rutile (see Fig. 2 for locations of trapping sites). In surface layers hole stabilisation energies oscillate and within 1-2 nm below the surface the profiles converge to the bulk value  $\epsilon_T^B$ . With exception of rutile {100} surface the most stable hole states are localized on surface bridging oxygen sites.

After electronic and atomic structures relaxation the total magnetic moment assumed value close to 1.0 (spin 1/2) with spin density localized on the oxygen site hosting the hole. The electron remains delocalized over two spin channels. Only in case of rutile (001) surface the total magnetic moment was somewhat larger (between 1.0 and 1.8) and the additional spin density originated from the electron localization on Ti atoms on the non-relaxed part of the slab.

The delocalized state of the electron minimizes the interaction with the localized hole and renders it independent on the position of the hole. Such situation is desirable as photo-generated electron-hole pairs separation precedes photocatalytic processes<sup>5</sup>.

## References

- 1 P. Zawadzki, K. W. Jacobsen and J. Rossmeisl, *Chem. Phys. Lett.*, 2011, **506**, 42 – 45.
- 2 A. Ruzsinszky, J. P. Perdew, G. I. Csonka, O. A. Vydrov and G. E. Scuseria, *J. Chem. Phys.*, 2007, **126**, 104102.
- 3 P. Mori-Sanchez, A. J. Cohen and W. Yang, *Phys. Rev. Lett.*, 2008, **100**, 146401.

<sup>a</sup> Center for Atomic-Scale Materials Design, Department of Physics, Technical University of Denmark, DK-2800 Kgs. Lyngby, Denmark

<sup>b</sup> Center for Individual Nanoparticle Functionality, Department of Physics, Technical University of Denmark, DK-2800 Kgs. Lyngby, Denmark

<sup>§</sup> Present address: National Renewable Energy Laboratory, Golden, Colorado 80401, USA

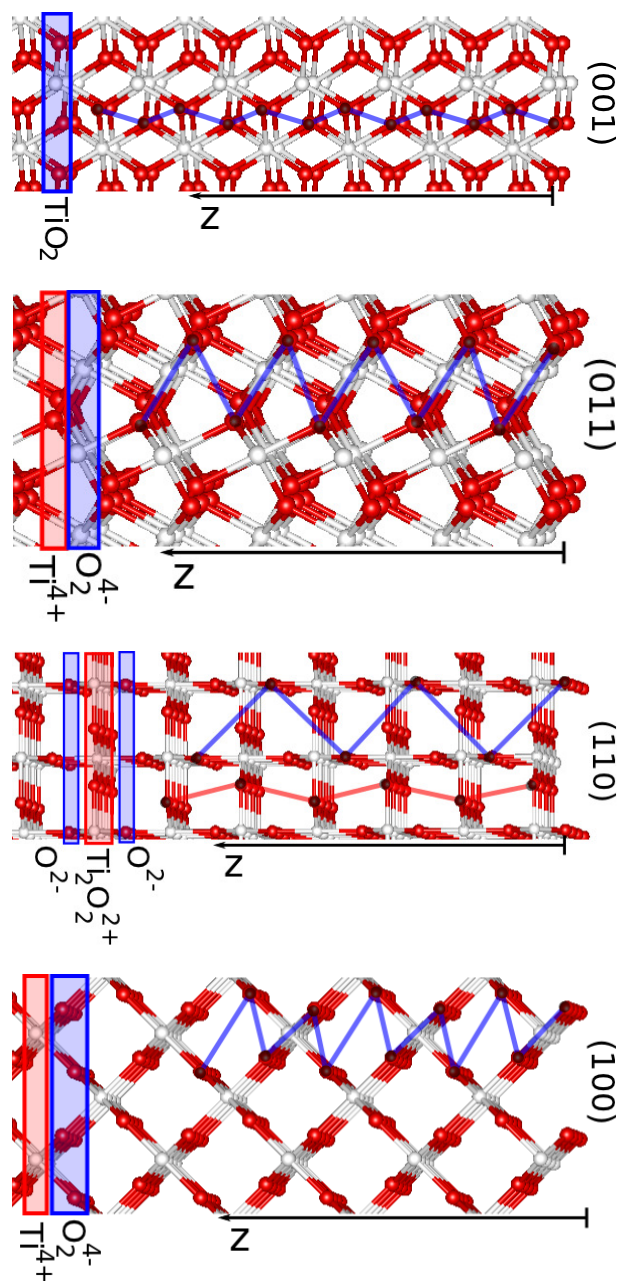


**Fig. 2** Rutile surfaces. Blue and red lines link the hole trapping sites for which the hole stabilisation energies are plotted on Fig. 1.

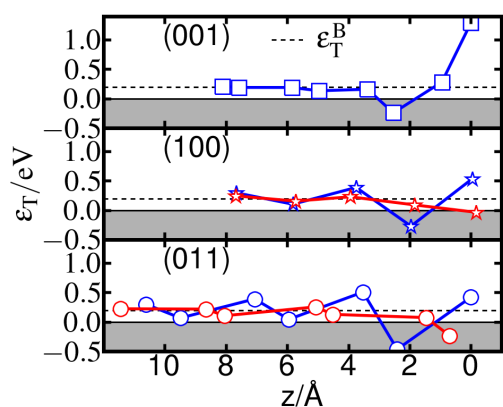


**Fig. 3** Self trapping energies  $\epsilon_T$  with respect to the valence band edge for anatase (see Fig. 4 for locations of trapping sites). In surface layers hole stabilisation energies oscillate and within 1-2 nm below the surface the profiles converge to the bulk value  $\epsilon_T^B$ .

- 4 J. Gavnholt, T. Olsen, M. Englund and J. Schiøtz, *Phys. Rev. B*, 2008, **78**, 075441.  
 5 M. A. Henderson, *Surf. Sci. Rep.*, 2011, **66**, 185–297.

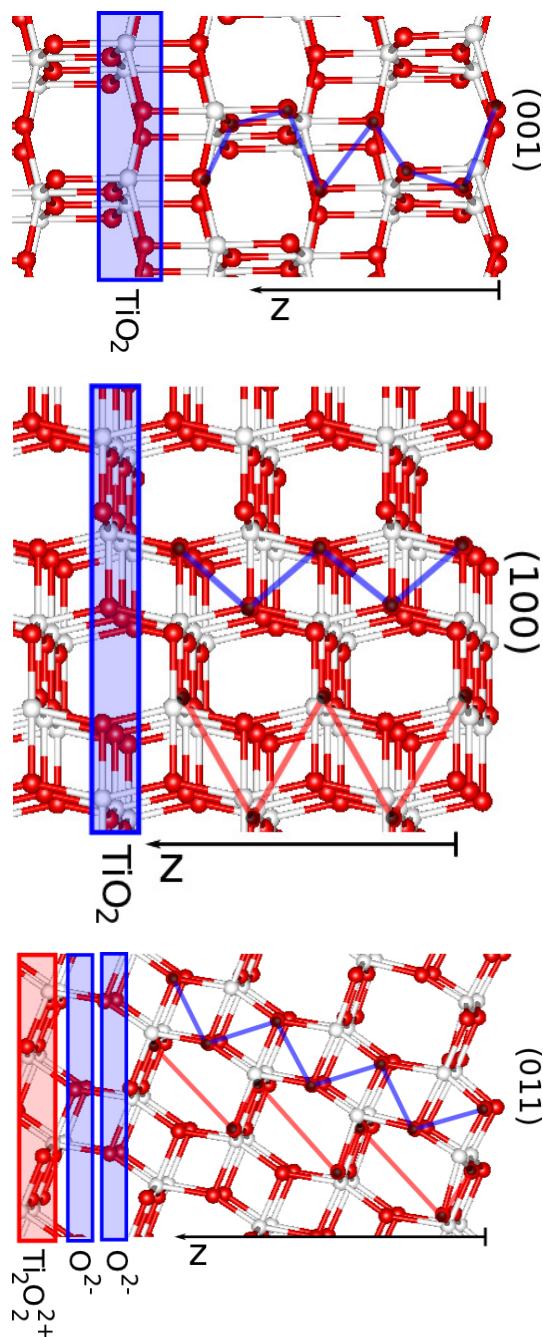


**Fig. 4** Anatase surfaces. Blue and red lines link the hole trapping sites for which the hole stabilisation energies are plotted on Fig.3.

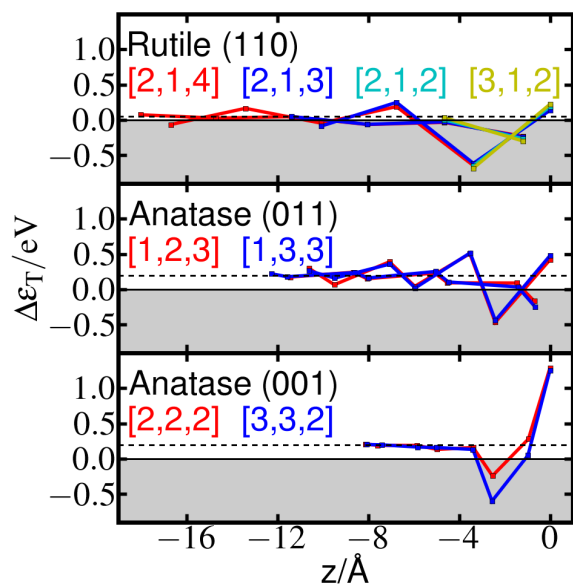


Fig. 5 Self-trapping energies  $\epsilon_T$  calculated with different cell sizes.

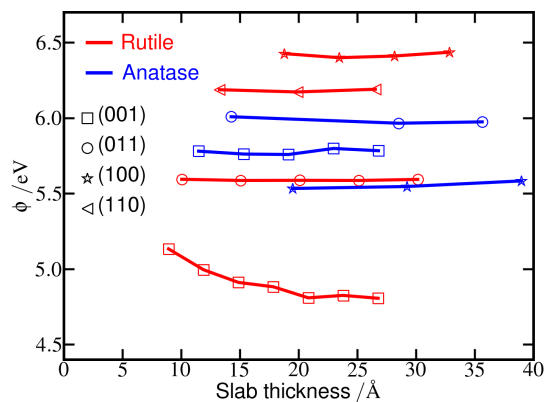


Fig. 6 Convergence of the work function with the slab thickness.